Removal of a Methyl Group Causes Global Changes in *p*-Hydroxybenzoate Hydroxylase[†,‡]

Lindsay J. Cole,[§] Domenico L. Gatti,[‖] Barrie Entsch,[§] and David P. Ballou*,[§]

Department of Biological Chemistry, University of Michigan, Ann Arbor, Michigan 48109-0606, and Department of Biochemistry and Molecular Biology, Wayne State University, Detroit, Michigan 48201

Received January 19, 2005; Revised Manuscript Received April 11, 2005

ABSTRACT: *p*-Hydroxybenzoate hydroxylase (PHBH) is a homodimeric flavoprotein monooxygenase that catalyzes the hydroxylation of *p*-hydroxybenzoate to form 3,4-dihydroxybenzoate. Controlled catalysis is achieved by movement of the flavin and protein between three conformations, *in*, *out*, and *open* [Entsch, B., et al. (2005) *Arch. Biochem. Biophys. 433*, 297−311]. The *open* conformation is important for substrate binding and product release, the *in* conformation for reaction with oxygen and hydroxylation, and the *out* conformation for the reduction of FAD by NADPH. The *open* conformation is similar to the structure of Arg220Gln-PHBH in which the backbone peptide loop of residues 43−46, located on the *si* side of the flavin, is rotated. In this paper, we examine the structure and properties of the Ala45Gly-PHBH mutant enzyme. The crystal structure of the Ala45Gly enzyme is an asymmetric dimer, with one monomer similar (but not identical) to wild-type PHBH, while the other monomer has His72 flipped into solvent and replaced with Glu73 as one of several changes in the structure. The two structures correlate with evidence from kinetic studies for two forms of Ala45Gly-PHBH. One form of the enzyme dominates turnover and hydroxylates, while the other contributes little to turnover and fails to hydroxylate. Ala45Gly-PHBH favors the *in* conformation over alternative conformations. The effect of this mutation on the structure and function of PHBH illustrates the importance of the *si* side loop in the conformational state of PHBH and, consequently, the function of the enzyme. This work demonstrates some general principles of how enzymes use conformational movements to allow both access and egress of substrates and product, while restricting access to the solvent at a critical stage in catalysis.

p-Hydroxybenzoate hydroxylase (PHBH)[1] is a single-component flavoprotein monooxygenase that catalyzes the incorporation of an atom of dioxygen into *p*-hydroxybenzoate (pOHB) to form 3,4-dihydroxybenzoate (3,4DOHB). The catalytic mechanism of PHBH (Figure 1) is the model for a large family of flavoprotein hydroxylases (*1*, *2*), and the function of the protein in this mechanism is supported by an extensive large collection of crystal structures of the wild-type (WT) and mutant forms of this enzyme. Analysis of the relationships between structure and function in PHBH has illuminated the role of conformational movements that are important in catalysis in this family of enzymes (*2*). The enzyme is a homodimer with a monomer molecular mass of 45 kDa. There is one FAD per monomer, and each active site is composed of residues from one monomer only. In PHBH, the isoalloxazine of the FAD moves between two different positions to carry out two different reactions at sites that are near each other on a single polypeptide. At least three distinct conformational states play important roles in substrate binding and product release, reaction and interaction with NADPH, and the reactions with molecular oxygen.

The crystal structure of the Arg220Gln mutant enzyme (*3*) in the presence and absence of pOHB has been determined to 2.0 Å resolution. In the crystal, this variant adopts a unique conformation, called the *open* structure, in which the substrate-binding domain of the protein has moved away from the other two domains to allow substrate access to the active site. This *open* structure models a conformation involved in the initial binding of substrate (*3*) that would be followed by a shift in equilibrium to the closed or *in* form represented by the WT structure with pOHB bound (*4*).

If one starts with the oxidized enzyme, pOHB and NADPH must bind before initiation of reduction of the flavin. NADPH and pOHB can bind in any order, but pOHB must be bound for fast hydride transfer from NADPH to flavin to proceed (*5*, *6*). This is the key catalytic control point for this reaction cycle, which is exergonic and irreversible. If the flavin were reduced without pOHB, it would react with oxygen and eliminate H_2O_2 (k_{10}, Figure 1), a destructive oxidant that can be damaging to the cell. This futile cycle also wastefully consumes NADPH. For flavin reduction to occur in the

[1] Abbreviations: PHBH, *p*-hydroxybenzoate hydroxylase; WT-PHBH, normal *p*-hydroxybenzoate hydroxylase; Ala45Gly-PHBH, mutant form of *p*-hydroxybenzoate hydroxylase; pOHB, *p*-hydroxybenzoate; 2,4DOHB, 2,4-dihydroxybenzoate; 3,4DOHB, 3,4-dihydroxybenzoate; CHES, 2-(*N*-cyclohexylamino)ethanesulfonic acid.
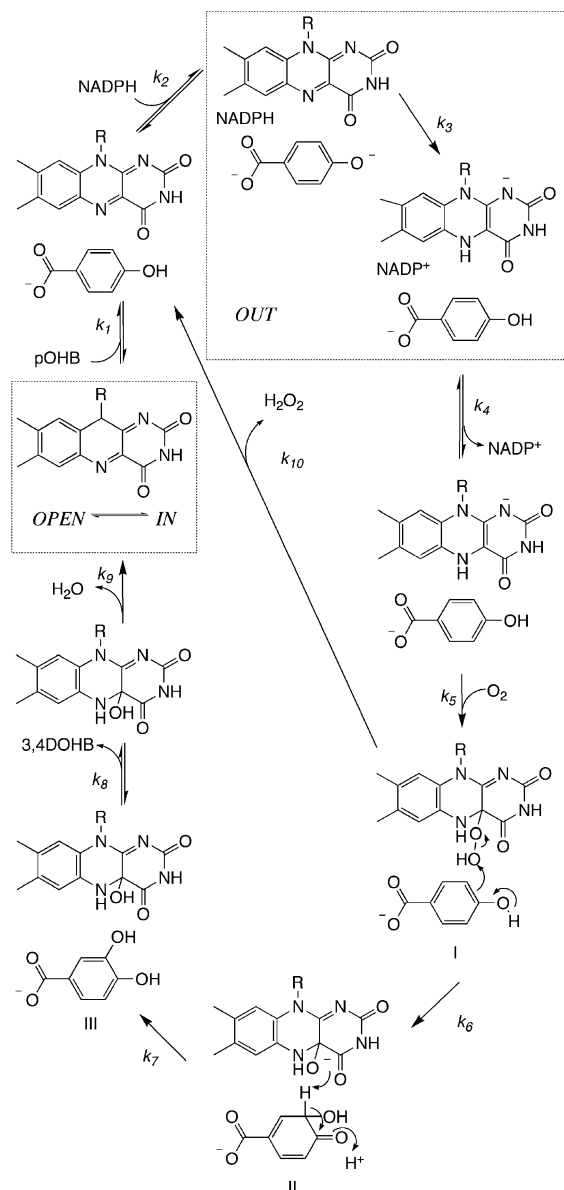
FIGURE 1: Catalytic cycle of PHBH. Three oxygen reaction intermediate states are labeled as intermediates **I**, **II**, and **III**. The steps that requires the *open* and *out* conformations of the enzyme are boxed and labeled, while the other steps take place in the *in* conformation.

enzyme, the flavin must move to the *out* position (*6*, *8*, *9*), where its exposure to solvent permits NADPH to approach and interact with N5 of the flavin for effective hydride transfer (*10*). The shift to the *out* conformation is triggered by deprotonation of the substrate phenolic oxygen (*6*) facilitated by a H-bond network consisting of Tyr201, Tyr385, two waters, and His72 (*11*, *12*). When the phenolic oxygen of pOHB is deprotonated, the resulting negative charge on the phenolic oxygen exerts a charge-to-dipole force upon the backbone carbonyl of Pro293 (*11*), causing a slight rotation of this rigid loop (Pro292, Pro293, and Thr294) to favor the *out* conformation where the FAD is reduced.

Upon formation of reduced flavin, the anionic isoalloxazine moves back to the *in* conformation because of the positive electrostatic field of the active site (*13*, *14*). In the *in* conformation, the flavin is isolated from solvent and oriented appropriately toward the substrate for hydroxylation to occur. Reaction with oxygen to form a stable hydroper-

oxide (intermediate **I**, Figure 1) can only occur when the flavin is isolated from attack by water (*15*). Molecular oxygen enters the active site, reacts with reduced flavin, and obtains a proton to form the flavin−C4a-hydroperoxide intermediate. pOHB is activated for a nucleophilic displacement of the distal oxygen of the flavin−C4a-hydroperoxide intermediate by deprotonation of the phenolic oxygen. The hydroxylation reaction results in a nonaromatic dienone intermediate (Figure 1, intermediate **II**) along with the flavin−C4a-hydroxide intermediate. Intermediate **II** rapidly re-aromatizes to form the final product, 3,4DOHB, which is released along with water from the flavin−C4a-hydroxide intermediate when the enzyme shifts to the *open* conformation.

Ala45 in PHBH is located on the *si* side of the isoalloxazine of FAD, and its methyl group is in van der Waals contact with the C4a position (Figure 2). Ala45 is in the center of a loop containing Arg42, Arg44, Ala45, Gly46, Leu48, and Glu49, which are all highly conserved in PHBH across species. The peptide backbone of the neighboring Arg44 is strained when in the *in* conformation (*16*, *17*). This strain may be part of the driving force for movement of the side chain of Arg44 to allow flavin to swing *out*. Arg44 is also involved in binding the 2′-phosphate of NADPH (*3*).

In the crystal structure of Arg220Gln-PHBH (*3*), the *si* side loop from residue 43 to 49 is rotated almost 180° compared to that of the WT to form the *open* structure (Figure 2). The unfavorable backbone conformation of Arg44 is completely relieved [analysis of the published structure by Wang et al. (*3*)]. The highly conserved Arg44 and Ala45 residues are conspicuously placed right in the center of the "machinery" for this conformational change in the enzyme. In this report, we have investigated the role of Ala45 and the flavin *si* side loop of PHBH using site-directed mutagenesis to change Ala45 to glycine, to create a flexible Gly-Gly backbone with Gly46. Significant structural changes occurred. In the crystal, one monomer had only minor differences compared to the WT structure, but the other monomer showed a large disturbance to the loop of residues 60−75, including a rotation of His72 into the solvent. The two different monomers observed in the crystal structure correlate well with the two distinctly different forms of Ala45Gly observed in solution. One form of the enzyme is a competent hydroxylase, but the second form is very slow in catalysis and is not an effective hydroxylase. The mutant enzyme also exhibited several other properties that have further elucidated our understanding of protein function. For example, the *in* conformation is more stable than in WT and is favored over the *open* and *out* conformations, thus demonstrating an important role of the *si* side loop in the balance between conformational states.

MATERIALS AND METHODS

All common reagents used in this work were analytical reagent grade. NADPH was at least 98% pure (purchased from Sigma). Other substrates for PHBH were from commercial sources and were recrystallized before use. (4R)-[4-²H]NADPH (NADPD) was prepared as previously described (*6*).

The construction of plasmids and the methods for expression of PHBH in *Escherichia coli* have been described
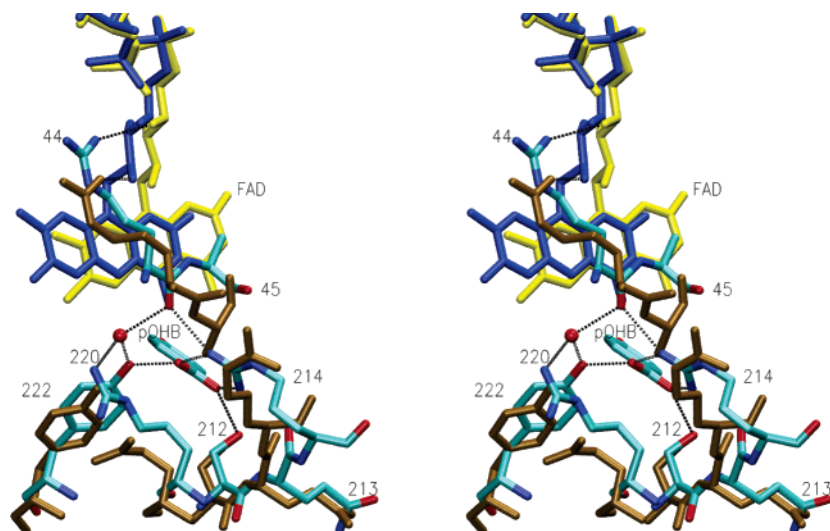
FIGURE 2: Stereodiagram of an overlay of the active site of WT-PHBH in complex with pOHB [the *in* conformation; Schreuder et al. (*4*); PDB entry 1PBE] and the structure of the substrate-free Arg220Gln mutant enzyme [the *open* conformation; Wang et al. (*3*); PDB entry 1K0L]. The protein residues of WT-PHBH are shown with cyan carbons, while the FAD is colored yellow. For the Arg220Gln structure, the protein residues are represented as brown bonds with the FAD shown as blue bonds. Significant H-bonds are shown as black dotted lines. The view shows that in the WT-PHBH structure, the side chains of Arg44 and Ala45 in the loop on the *si* side are closely associated with the flavin. The side chain of Arg44 H-bonds to the 3′-OH of the ribityl chain of FAD, while the methyl side chain of Ala45 is in van der Waals contact with the isoalloxazine ring. This view also shows the network of residues that bind to the carboxylate of pOHB and form H-bonds with the backbone carbonyl of Arg44 in the WT structure. In this structure, the peptide backbone of Arg44 is in a strained conformation. In the Arg220Gln mutant form of PHBH, the view shows the rotation of the peptide loop containing residues Arg44 and Ala45 compared to the WT structure; this rotation relieves the strained peptide backbone conformation of Arg44. This view of PHBH without the substrate also shows the large movement of the side chain of Arg214 compared to when the substrate is present in the active site, and the consequent elimination of a number of H-bonds to the carboxyl of the substrate and Arg44 present in the structure of WT-PHBH in complex with pOHB.

previously (*7, 18, 19*). Mutagenesis was carried using the QuikChange site-directed mutagenesis kit developed by Stratagene. The oligonucleotide primer pair sequence used to introduce the Ala45Gly mutation in the mutagenesis reaction was GGCCGCATCCGCGGCGGCGTGCTGG in the coding strand and its complement; underlined is the changed nucleotide. The WT and Ala45Gly forms of PHBH were isolated and purified as described in refs *7* and *20*. Residual substrate from the purification procedure remained bound to the Ala45Gly enzyme after purification. Removal of pOHB, where necessary, was achieved by turnover reactions of the enzyme with a >50-fold excess of NADPH in air-saturated buffer for >1 h at room temperature, followed by removal of products from the enzyme by use of a gel filtration column.

Quantification of 3,4DOHB for hydroxylation coupling measurements was achieved by separation of the reaction components on a Synergi polar-RP HPLC column (Phenomenex) using an isocratic mobile phase of 20% methanol and 1% acetic acid at a flow rate of 1 mL/min, monitoring the absorbance at 250 nm, and correlating the area to know standards of 3,4DOHB.

All experimental measurements with PHBH were carried out at 4 °C, except where noted, to slow reactions and facilitate quantitative analysis. For pH values of 6.5 and 7.0, 50 mM potassium phosphate buffer was used, and for pH values of 8.5−9.0, 50 mM Tris-SO$_4$ buffer was used. The measurements of ligand dissociation constants, pK_a values of pOHB bound to the enzyme, extinction coefficients, and redox potentials of the enzyme were carried out as described by Entsch et al. (*18*) and Moran et al. (*13*). All kinetic data were collected with a Hi-Tech Scientific model SF-61 stopped-flow spectrophotometer in either absorbance or

Table 1: Crystallographic Data and Refinement Statistics for Ala45Gly-PHBH

space group	$P2_12_12$
resolution (Å)	31.6−2.0
no. of measurements	779526
no. of unique reflections	59975
⟨redundancy⟩	13.0
completeness (%)	99.7
$\langle I\rangle/\sigma\langle I\rangle$	5.65
$R_{merge}{}^a$ (%)	8.0
$R_{cryst}{}^b$ (%)	22.1
$R_{free}{}^c$ (%)	26.8
no. of solvent molecules	542
$\langle B\rangle^d$ (Å^2)	36.9
rmsd for bond lengths (Å)	0.006
rmsd for bond angles (deg)	1.3
rmsd for dihedrals (deg)	22.9
rmsd for impropers (deg)	0.79
σA coordinate error (Å)	0.28

^{a} $R_{merge} = \sum_h\sum_i|I(h)_i - \langle I(h)\rangle|/\sum_h\sum_i|I(h)_i|$, where $I(h)_i$ is the *i*th measurement. ^{b} $R_{cryst} = \sum|F_{obs} - F_{calc}|/\sum|F_{obs}|$. ^{c} R_{free} was calculated on 10% of the data omitted from refinement. ^{d} Mean *B* values were calculated from the refined models.

fluorescence mode. Rapid reaction kinetic traces were analyzed and simulated with Program A, an MS-DOS-based series of programs developed in our laboratory at the University of Michigan, and KISS (Kinetic Instruments Stopped-flow System). Analysis is based upon the Marquardt algorithm for fitting data to sums of exponentials (*21*).

Crystallization, X-ray Data Collection, and Structure Refinement. Crystals of Ala45Gly-PHBH in complex with pOHB were obtained by vapor diffusion. Hanging drops containing 4 mg/mL enzyme in 100 mM Tris-SO$_4$ (pH 8.5) containing 40 μM FAD, 300 μM EDTA, 200 μM glutathione, 30 mM Na$_2$SO$_3$, and 500 μM pOHB were equilibrated for 2
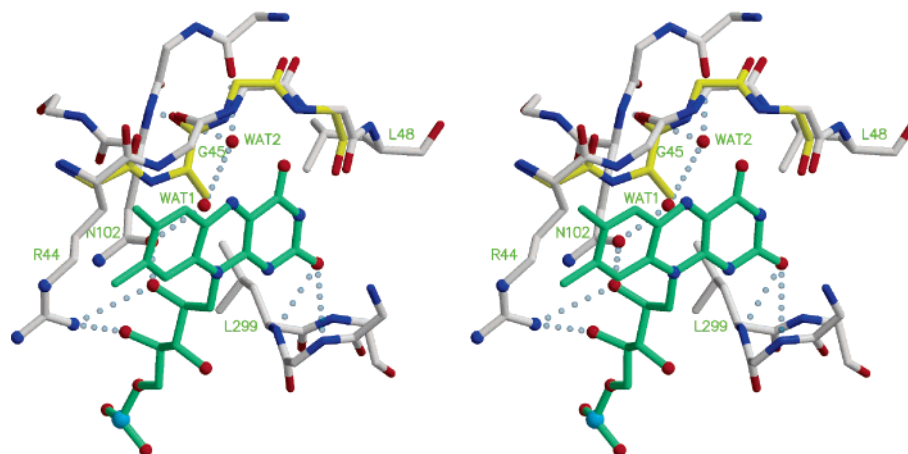
FIGURE 3: Stereoview of the active site of the WT-like monomer of Ala45Gly-PHBH around the site of the mutation. The structure of the wild-type enzyme in the region encompassing residues 44−47 is superimposed on the mutant. The backbone and side chains of the wild-type and Ala45Gly mutant enzyme are shown with yellow and ivory bonds, respectively; nitrogen is colored blue, and oxygen is colored red. The side chain of the wild-type Ala45 is replaced with a water molecule (WAT1). A second water molecule (WAT2) fills a nearby cavity delimited by the backbone of residues 101 and 102, and the side chains of Asn102, Leu48, and Leu299. FAD is shown with green bonds, its *re* face pointing toward the viewer. Hydrogen bonds are shown as dotted light blue lines. Coordinates for the wild-type enzyme are from PDB entry 1IUW.

weeks against a reservoir solution containing 35% saturated ammonium sulfate (at 37 °C). Rectangular yellow crystals were obtained with dimensions up to 0.5 mm × 0.2 mm. The crystals were exchanged into a holding solution of 50 mM Tris-SO$_4$ (pH 8.5) containing 20 μM FAD, 150 μM EDTA, 100 μM glutathione, 15 mM Na$_2$SO$_3$, 250 μM pOHB, 15% glycerol (v/v), and 50% saturated ammonium sulfate (at 37 °C), and the temperature was incrementally equilibrated to room temperature over the course of 4 h.

The diffraction data were collected from a single crystal at 100 K with an R-axis IV image plate detector at the Cu Kα wavelength. The protein crystallized as an asymmetric dimer in space group $P2_12_12$ and diffracted to 2.0 Å with the following unit cell dimensions: $a = 69.860$ Å, $b = 85.897$ Å, and $c = 146.074$ Å. The unit cell dimensions and space group are different from those of WT-PHBH. Consequently, the molecular replacement procedure was employed to determine the structure of the mutant enzyme. All steps were carried out using the CNS version 1.0 suite of crystallographic programs (*22*). Model refinement was carried out with CNS version 1.0 using the cross-validated maximum likelihood function as the target function. Solvent molecules were added during the final stages of refinement after the protein model had stabilized. The crystallographic data and refinement statistics are given in Table 1.

RESULTS

Structure of Ala45Gly-PHBH. Two monomers of Ala45Gly-PHBH with pOHB bound are present in the asymmetric unit of the crystal. The two monomers can be described as WT-like and His72-flipped. The structure of the WT-like monomer is similar to that of WT-PHBH with pOHB bound (*4*, *12*), and the perturbations within this structure are only in the region around the mutation. Replacement of Ala45 with Gly results in a small displacement of the backbone of Arg44, Gly45, and Gly46 away from the isoalloxazine (Figure 3). The methyl side chain of Ala45 in WT-PHBH is replaced with a water molecule (Wat1) that is within H-bonding distance (2.6 Å) of Gln102, and within 2.8 Å of

the C10a−C4a bond of the flavin (Figure 3). A second new water molecule (Wat2) further buried in the protein is ∼3.6 Å from Wat1. The close association of Wat1 with the bond between C4a and C10a is unusual; it is too close for a low-energy van der Waals interaction, but is consistent with H-bonding between the water and the conjugated π-electron system of the flavin, in a manner similar to aromatic H-bonds (*23*, *24*). This increase in the polarity of the environment around the flavin appears to affect the physical properties of the flavin bound to this mutant enzyme, and results in changes to the redox potential and spectral properties as described below.

The structure of the His72-flipped monomer of Ala45Gly-PHBH is very similar to the WT-like monomer around the loop of residues 42−49; with both, there is a similar rotation of the Gly45 backbone, and two waters replace the missing methyl side chain (not shown). However, the His72-flipped structure has extensive perturbations extending from residue 60 to ∼75 (Figure 4). These structural perturbations occur in a region of the protein that is 13−20 Å from the mutated residue, whereas there are only minor structural perturbations close to the mutation. The side chain of Glu73 occupies the position of the side chain of His72 in the WT structure, while the side chain of His72 is flipped out into solvent by almost 180° compared to its position in the WT enzyme. This shuffle of residues displaces the backbone from residue 72 to residue 76 (Figure 4). Furthermore, to accommodate the exchange of His72 with Glu73, a small α-helix (helix H4, residues 63−68 in the WT enzyme) is unwound and becomes partially disordered (in Figure 4A, notice the chain break in the mutant). The movement of His72 into the solvent also disrupts the H-bond network involving Tyr201, Tyr385, and two water molecules that is important in deprotonating the phenolic oxygen of the substrate in the active site during catalysis (Figure 4B; see also refs *6* and *12*).

The dimer interface between the two different forms of Ala45Gly-PHBH has one significant difference from WT-PHBH. The guanidinium of Arg179 of the WT-like monomer of Ala45Gly-PHBH is within charge-pairing distance of
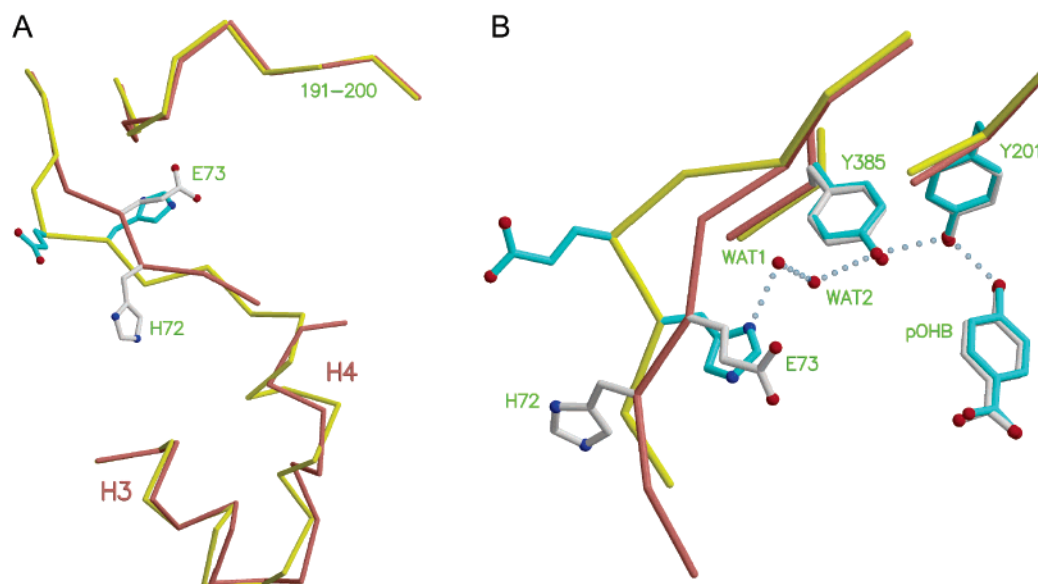
FIGURE 4: (A) Structure of the H72-flipped monomer of the Ala45Gly mutant of PHBH around His72. The Cα chains of the wild-type and mutant enzymes are shown in yellow and salmon bonds, respectively. Wild-type and mutant side chains are shown with cyan and ivory bonds, respectively. (B) Close-up view of the His72/Glu73 swap region. Rotation of His72 by ~180° in the mutant enzyme disrupts the network of hydrogen bonds involving two water molecules (WAT1 and WAT2), Tyr385, Tyr201, and substrate pOHB. Colors are the same as in panel A. Coordinates for the wild-type enzyme are from PDB entry 1IUW. WAT1 appears only under conditions that stabilize the H-bond network, like those present when the alternate substrate *p*-aminobenzoate is bound. Therefore, coordinates for WAT1 are from the structure of the wild-type enzyme in complex with *p*-aminobenzoate (PDB entry 1IUT).
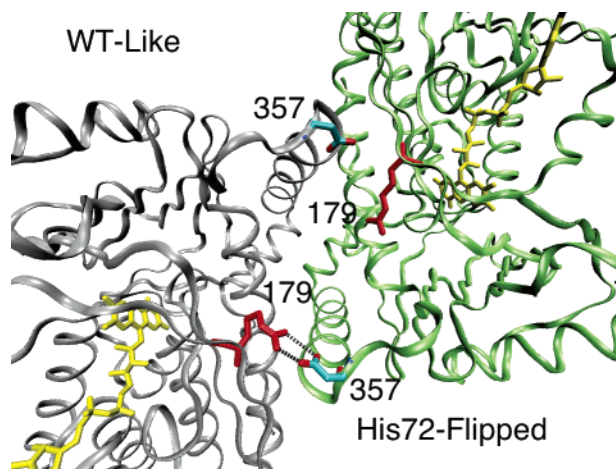

FIGURE 5: Dimer interface of Ala45Gly-PHBH. Residues Arg179 (red bonds) and Asp357 (cyan carbons) from both monomers of the dimer of Ala45Gly-PHBH are shown along with both FAD molecules (yellow bonds) and the backbone of the WT-like monomer (gray ribbon) and the His72-flipped monomer (green ribbons). Residue Arg179 of the WT-like monomer is within hydrogen bonding distance (black dotted lines) of Asp357 of the His72-flipped monomer (not observed in WT-PHBH). Arg179 of the His72-flipped monomer is not close to Asp357, but points out into a solvent cavity between the monomers (as observed in WT-PHBH).

Asp357 in the His72-flipped monomer (Figure 5). Arg179 in WT-PHBH, and in the His72-flipped monomer, does not interact with Asp357 of the other monomer, but instead points out into a solvent cavity between the monomeric subunits.

Some Properties of Ala45Gly-PHBH. The absorption spectrum of the mutant enzyme was different from that of the WT enzyme, with a shift of the visible peak from 450 nm (extinction coefficient of 10.3 mM^{-1} cm^{-1}) to 444 nm (extinction coefficient of 9.8 mM^{-1} cm^{-1}) (Table 2).

Moreover, the spectrum of the mutant enzyme is not dependent upon pH, unlike the spectrum of the WT enzyme. The binding of Ala45Gly-PHBH with substrates and substrate analogues showed significant differences from the binding of the WT enzyme. The ligands, pOHB ($K_d = 0.7 \pm 0.07$ μM) and 3,4DOHB ($K_d = 14 \pm 1$ μM), both bound with higher affinity to the Ala45Gly enzyme than to the WT enzyme (Table 2). It has been found that specific changes in the spectrum of the flavin upon binding substrates in the active site are associated with specific conformational states of the enzyme (*2, 17*). The spectral perturbations of FAD in Ala45Gly-PHBH upon binding pOHB and 3,4DOHB (product) at pH 6.5 are both similar to the characteristic pOHB difference binding spectrum for the WT enzyme (Figure 6), suggesting that the flavin is in the *in* conformation at equilibrium with these ligands. The WT enzyme does not form exclusively the *in* conformation when in a complex with the product, 3,4DOHB, but forms an equilibrium between conformational states. Thus, product dissociates from the WT enzyme at a rate suitable for catalysis, but more slowly from Ala45Gly-PHBH. At pH 6.5, Ala45Gly-PHBH binds 2,4DOHB with a K_d of 2200 ± 200 μM, indicating a much lower affinity than for the WT enzyme (Table 2). Spectral perturbations of Ala45Gly-PHBH upon binding of 2,4DOHB were similar to those of the WT enzyme with 2,4DOHB, a higher-extinction, less resolved spectrum characteristic of the *out* conformation of flavin (refs *1* and *17* and Figure 6). The *out* conformation of the WT enzyme is stabilized by new interactions developed with 2,4DOHB bound (*17*). It appears that the same interactions in the Ala45Gly enzyme are not enough to counter the extra stability of the *in* conformation.

In the catalytic cycle of PHBH, formation of the phenolate form of pOHB in the active site is one of the prerequisites for both hydroxylation and hydride transfer from NADPH (*6, 25*). Deprotonation of the phenol of pOHB is facilitated

Table 2: Selected Properties of Ala45Gly-PHBH Compared to Those of WT-PHBH[a]

	WT	Ala45Gly-PHBH
% coupling with pOHB at pH 6.5 and 4 °C	100 ± 1	67[c] ± 2
% coupling with pOHB at pH 8.5 or 8.7 and 4 °C	86[d] ± 1 at pH 8.7	90[b] ± 5, 55[c] ± 5 at pH 8.5
K_d (μM) with pOHB at pH 6.5 and 4 °C	9.5 ± 0.5	0.7 ± 0.05
K_d (μM) with 2,4DOHB at pH 6.5 and 4 °C	22 ± 1.5	2200 ± 200
K_d (μM) with 3,4DOHB at pH 6.5 and 4 °C	230 ± 15	14 ± 0.5
pK_a of the 4-OH of pOHB bound to the enzyme	7.4 ± 0.1	>9.0
k_{cat} (s^{-1}) at pH 6.5 and 4 °C	5.7 ± 0.2	0.06 ± 0.01
k_{cat} (s^{-1}) at pH 8.5 or 8.6 and 4 °C	7.5[d] ± 0.2 at pH 8.6	1.1 ± 0.2 at pH 8.5
$E°'$, free enzyme (mV)	−163 ± 1.5	−186 ± 1.5
$E°'$, enzyme with pOHB (mV)	−165 ± 1.5	−193 ± 1.5
E_{ox}, visible peak (no ligand)	ϵ_{450} = 10.3 mM^{-1} cm^{-1}	ϵ_{444} = 9.8 mM^{-1} cm^{-1}

[a] All experimental results were determined as described in Materials and Methods. WT data were obtained from ref *18* unless otherwise noted. [b] Hydroxylation coupling was assessed by steady-state turnover of the mutant enzyme with excess NADPH and air-saturated buffer, correlating consumption of NADPH with production of 3,4DOHB (measured after separation from other reaction components using reverse phase HPLC). [c] Hydroxylation coupling was assessed by a single turnover of the dithionite-reduced Ala45Gly-PHBH enzyme with excess pOHB and oxygen, correlating the concentration of 3,4DOHB (measured by separation from other reaction components using reverse phase HPLC) produced to the concentration of enzyme reacted. [d] Value from ref *14*.
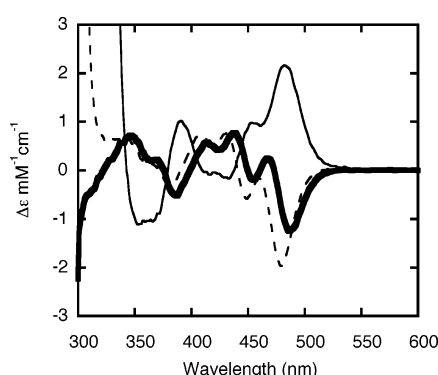

FIGURE 6: Absorption difference spectra of FAD obtained from titrations of Ala45Gly-PHBH with ligands at pH 6.5 and 4 °C. The difference spectra represent nearly saturating concentrations of pOHB (thick solid line), 2,4DOHB (thin solid line), and 3,4DOHB (dashed line). $\Delta\epsilon$ = extinction of the bound enzyme − extinction of the free enzyme.

by a H-bond network that connects the 4-hydroxyl of pOHB to solvent (*12, 26, 27*). In solution, the pK_a of the pOHB 4-hydroxyl is 9.3, whereas when it is bound to the WT enzyme, it is 7.4 (*18*). The extinction coefficient of the phenolate form of pOHB is 17 300 M^{-1} cm^{-1} at 280 nm, and phenolate absorbance can be used to estimate the pK_a on the enzyme (*18*). At pH 9.5 (the highest pH at which the enzyme is stable), pOHB bound to Ala45Gly-PHBH is only partly deprotonated. By assuming the same extinction coefficient for the dianion of pOHB on the mutant enzyme as for the free substrate, we could fit a sigmoidal curve to the pH-dependent spectral changes to give a pK_a of ~9.0 (certainly ≥9.0), a value similar to that of the free substrate. Therefore, the H-bond network in Ala45Gly-PHBH is unable to lower the pK_a of the phenol of pOHB below that of free solution.

Redox potential determinations of Ala45Gly-PHBH were carried out with both the free enzyme and the enzyme in complex with pOHB. The potentials of Ala45Gly-PHBH are lower than those of WT-PHBH for substrate-free (by 23 mV) and pOHB-bound enzymes (by 28 mV) as shown in Table 2. This decrease in redox potential may be due to the extra water molecules near the flavin that are observed in the crystal structure described above (Figure 3).

With WT-PHBH, the fraction of product formed from pOHB per reduced FAD oxidized is the same whether

NADPH is used to reduce the enzyme during turnover or the complex of the reduced enzyme with pOHB is reacted with oxygen (a single half-reaction). This ratio is 1 between pH 6 and 7 for WT, and declines slightly at higher pH (Table 2). With Ala45Gly-PHBH, the fraction of product formed is complex and depends on whether single-turnover or steady-state reactions are carried out. At pH 6.5, the enzyme turns over so slowly (largely because of the slow reductive half-reaction; see below) that the fraction of enzyme forming product cannot be measured accurately during turnover. When measured in an oxidative half-reaction, the ratio is 0.67 (Table 2). At pH 8.5, where turnover can be assessed, the fraction measured during turnover (0.9, similar to that of WT) is quite different from that measured in an oxidative half-reaction (0.55). A model that explains this discrepancy in results is presented in Oxidative Half-Reaction.

Reductive Half-Reaction. The reduction of PHBH ($k_2−k_4$ in Figure 1) can be followed in a stopped-flow spectrophotometer by mixing the anaerobic oxidized Ala45Gly enzyme complexed with pOHB with anaerobic solutions of NADPH and substrate. When the reaction was carried out at pH 6.5 and 4 °C (conditions widely used to study PHBH) and the reaction was monitored at 450 nm, a slow biphasic reduction process was observed (Figure 7A). Both phases exhibited a dependence on NADPH concentration. The dependence upon NADPH concentration was used to determine the value of k_3 in Figure 1 as described previously (*10*). The faster (k_3 = 0.076 ± 0.007 s^{-1}, $K_{d,NADPH}$ = 900 ± 90 μM) of the two processes was dominant, accounting for 80% of the total change. Enzyme in the second phase was reduced even more slowly (k_3 = 0.003 ± 0.0005 s^{-1}, $K_{d,NADPH}$ = 1800 ± 200 μM). For comparison, under the same conditions, WT-PHBH reduces in a single phase with a rate constant of 50 s^{-1}.

Reductive half-reactions of Ala45Gly-PHBH were repeated at several pH values; the reactions at pH 8.5 and 4 °C are shown in Figure 8A. At pH 8.5, the reaction was different from that at pH 6.5 and from that of the WT enzyme. Absorbance traces at pH 8.5 showed an increase in the reaction rate and an increase in the complexity of the reaction to three phases (Figure 8A). Analysis of the dependence of the fastest phase on NADPH concentration gave a rate constant for reduction of 7.0 ± 0.3 s^{-1} ($K_{d,NADPH}$ = 1000 ± 100 μM, 64% of the total amplitude); the second
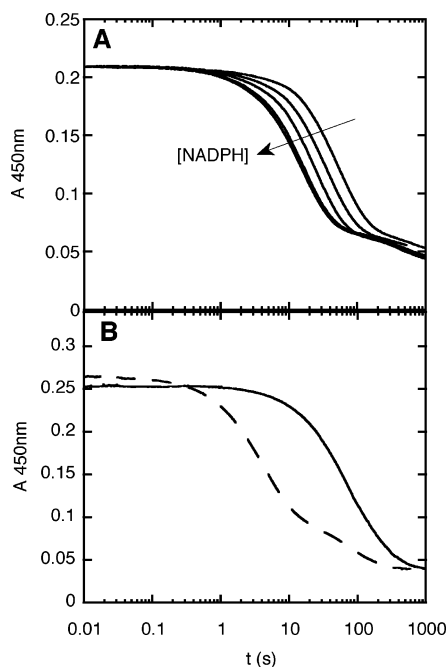
FIGURE 7: Reduction of Ala45Gly-PHBH in complex with pOHB at pH 6.5. (A) Stopped-flow reaction traces of the reduction process monitored at 450 nm, pH 6.5, and 4 °C under anaerobic conditions with 21 μM enzyme in complex with pOHB (500 μM) and NADPH concentrations of 275, 460, 790, 2585, and 4820 μM. The reduction kinetics were analyzed as described by Ortiz-Maldonado et al. (*10*). The traces were biphasic and could be fitted by two parallel exponentials with a residual of <0.002 AU. (B) NADPD kinetic isotope effect on reduction of Ala45Gly-PHBH at pH 6.5 and 25 °C. Ala45Gly-PHBH (final concentration of 25 μM) was complexed with pOHB (500 μM) and reacted with various concentrations of NADPD (final concentration of 5.4 mM shown as the solid line) or NADPH (final concentration of 5.1 mM shown as the dashed line). The reaction kinetics were analyzed as described above. Two phases of reduction by NADPD were observed, though they are much closer in rate than with NADPH. The faster of the two reduction reactions had a kinetic isotope effect of 10 $\pm$ 1, and the slower phase had a kinetic isotope effect of 2.5 $\pm$ 0.5.

phase gave a rate constant for reduction of 0.25 $\pm$ 0.02 s^{-1} (no dependence on NADPH concentration, 12% of the total amplitude), and finally, the slowest phase gave a rate constant of 0.08 $\pm$ 0.008 s^{-1} ($K_{d,NADPH}$ = 3700 $\pm$ 300 μM, 24% of the total amplitude). Compared to the results at pH 6.5, there was a higher proportion of the slowest form and a lower proportion of the fastest form. The intermediate phase shows no observable NADPH dependence, and represents a portion of enzyme that has to undergo a rate-determining conformational change before reduction can occur. This conformational change is possibly conversion to the faster-reducing form, similar to the interconversion observed in pH-jump experiments described below. For comparison, at pH 8.5 the WT enzyme is reduced in a single phase with a rate constant of 80 s^{-1}. Thus, the fastest phase in the reduction of Ala45Gly enzyme is only ~10% of the WT rate.

To demonstrate the proposed interconversion between the fast and slowly reducing forms of the enzyme, a pH-jump, double-mixing stopped-flow experiment was performed. Anaerobic Ala45Gly-PHBH complexed with pOHB at pH 6.0 (10 mM potassium phosphate buffer) was mixed initially with an equal volume of CHES buffer (100 mM, pH 9.5) to give a final pH of 8.8 (50 mM CHES and 5 mM potassium phosphate) in the stopped-flow spectrophotometer. The
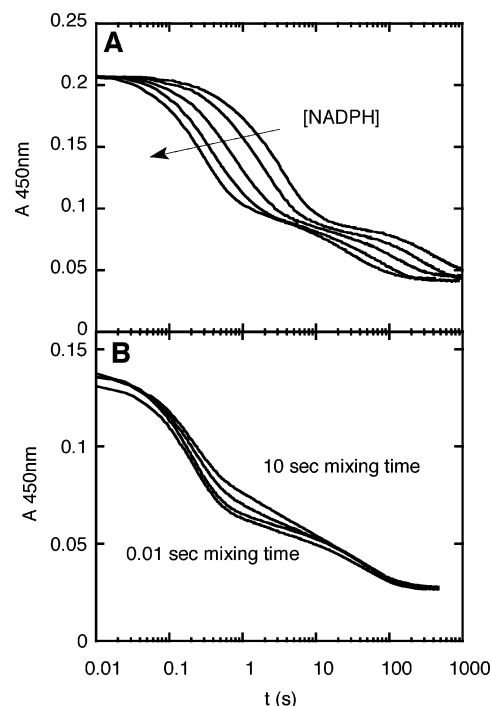

FIGURE 8: Reduction of Ala45Gly-PHBH complexed with pOHB at pH 8.5. (A) Stopped-flow reaction traces of the reduction process carried out anaerobically with 21 μM enzyme in complex with 500 μM pOHB at 450 nm and 4 °C, with NADPH concentrations of 100, 200, 400, 800, and 1600 μM (all concentrations are after mixing). The reaction traces were analyzed as described by Ortiz-Maldonado et al. (*10*), and could be fitted with three parallel exponentials, leaving a residual of <0.002 AU. Two phases exhibited a dependence on NADPH concentration, and the third was independent of NADPH concentration. (B) Double mixing stopped-flow reaction traces at 450 nm obtained by initially mixing the enzyme at pH 6.0 (final concentration of 14 μM in 5 mM phosphate buffer and 500 μM pOHB) with buffer at pH 9.5 (CHES final concentration of 50 mM) to give a final pH of 8.8. The enzyme solution was aged at pH 8.8 for times ranging from 10 ms to 100 s (10 ms, 100 ms, 1 s, and 10 s traces are shown), and then mixed with a solution of NADPH to give a final concentration of 1 mM. The change in amplitude of the second phase with time is a measure of the rate of approach to equilibrium between the different structural forms of the enzyme.

enzyme was aged at the higher pH for various periods ranging from 10 ms to 100 s before being mixed with NADPH in the second stage (final concentration of 1 mM) in the same final buffer (pH 8.8). As with single mixing experiments at pH 8.5, three distinct phases could be observed at all age times investigated (Figure 8B). The fastest phase had a constant observed rate of 4.5 $\pm$ 0.5 s^{-1}, but the fraction in this phase decreased from 66 to 51% of the total change as the enzyme aged at the higher pH. This change occurred at a rate of 1 $\pm$ 0.2 s^{-1}, as determined from analysis at various delay times. The second phase had a constant rate of 0.35 $\pm$ 0.04 s^{-1}, but the fraction occurring in this phase increased from 11 to 25% (also with an equilibration rate constant of 1 $\pm$ 0.3 s^{-1}). The last phase (0.02 $\pm$ 0.002 s^{-1} and 24% of the total change) remained constant with an increasing age time.

Deuterium Isotope Effects in Reduction. Anaerobic oxidized Ala45Gly-PHBH in complex with pOHB at pH 6.5 and 25 °C was reduced with different concentrations of NADPD, and the results were compared to results of similar experiments with NADPH (Figure 7B). The higher temper-
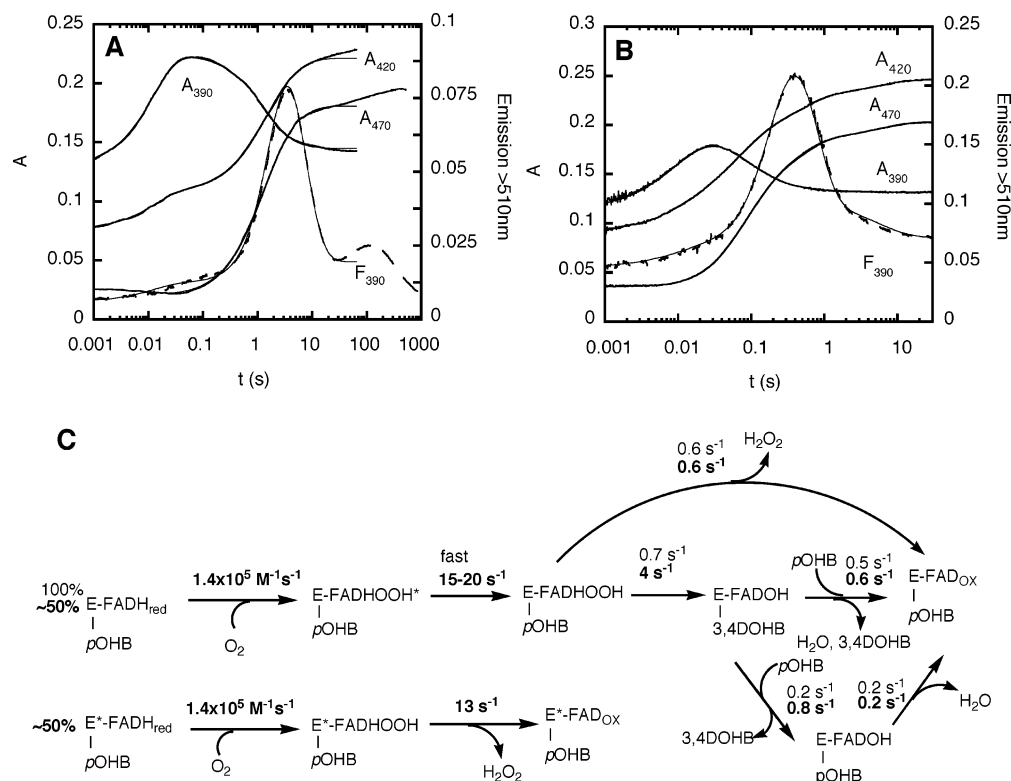
FIGURE 9: Oxygen half-reaction of Ala45Gly-PHBH in complex with pOHB. (A) Traces of absorbance (—) and fluorescence with excitation at 390 nm (— — —) from the reaction of reduced enzyme (25 μM in 50 mM potassium phosphate buffer at pH 6.5 and 4 °C) with 80 μM pOHB and 0.63 mM oxygen. Reaction traces could be fitted to five parallel exponentials with varying amplitudes across all wavelengths for both absorbance and fluorescence. The five phases can be clearly seen in the trace of fluorescence intensity. (B) Absorbance (—) and fluorescence with excitation at 390 nm (— — —) traces from the reaction of the reduced enzyme (30 μM) in complex with pOHB (500 μM) at pH 8.5 (50 mM Tris-SO$_4$) and 4 °C with 0.63 mM oxygen. (C) Model used to simulate the kinetic traces that are plotted over the data in panels A and B. The rate constants used for pH 6.5 (A) are listed above those for pH 8.5 (B), which are in bold. The slowest phases observed at pH 6.5, which are significantly slower than k_{cat}, have not been modeled.

ature (25 °C) compared to other studies with this enzyme was used because of the very slow reduction at pH 6.5 (see Figure 7A). If the rate-determining step in reduction is hydride transfer, the reduction rate constant should exhibit a large isotope effect as the deuterium is transferred from NADPD to flavin. Alternatively, if a slow conformational change or other event is rate-determining for reduction of flavin (with fast hydride transfer), the deuterium isotope effect should be small. The faster-reducing form of the Ala45Gly enzyme exhibits a full primary deuterium isotope effect of 10 ± 1 with NADPD ($K_{d,NADPD}$ = 4 ± 0.4 mM and $k_{red,NADPD}$ = 0.04 ± 0.005 s^{-1}, $K_{d,NADPH}$ = 4.2 ± 0.4 mM and $k_{red,NADPH}$ = 0.4 ± 0.02 s^{-1}), while the slower-reducing form exhibits an isotope effect of 2.5 ± 0.5. Thus, a conformational change is not a rate-determining step for reduction of the faster-reducing form of Ala45Gly-PHBH, while a conformational change may be rate-limiting for reduction of the slower-reducing form of Ala45Gly-PHBH.

Turnover Rates of Ala45Gly-PHBH. The overall catalytic reaction of the mutant enzyme was studied in the steady state by the enzyme-monitored turnover method (28), where the redox state of the FAD cofactor is monitored during the reaction. With limiting levels of oxygen (260, 440, and 750 μM) at pH 6.5 and 4 °C, and saturating levels of pOHB (10 mM) and NADPH (10 mM), the majority of FAD (~85%) is present in the oxidized form during turnover at the steady state. This high fraction of the oxidized enzyme occurs because the reduction of FAD is the slowest step in turnover. When the limiting concentration of oxygen is depleted, the

enzyme becomes fully reduced. During most of the reaction, there was no dependence upon substrate concentration or O$_2$ concentration until O$_2$ had almost been completely depleted, demonstrating a very low K_m for O$_2$ (<5 μM); therefore, the rate of turnover could be measured from the following equation:

$$ TN = \frac{[O_2]_{total}}{[Enz](\text{time taken to consume } O_2)} $$

From this relationship, a turnover rate of 0.06 ± 0.01 s^{-1} at pH 6.5 was obtained (Table 2). This is consistent with the 80% of the enzyme that is reduced in the faster phase (0.076 s^{-1}) being the primary determinant for the rate of catalysis. The experiment was repeated at pH 8.5 and 4 °C with 4 mM NADPH, 1 mM pOHB, and 260, 400, and 750 μM oxygen; a similar low K_m for O$_2$ was observed, and a turnover rate of 1.1 ± 0.2 s^{-1} was determined. At pH 8.5, reduction of FAD is not the rate-determining step for the fast-reducing form of the enzyme. However, turnover is more than 5-fold faster than the second phase in the reductive half-reaction and 50-fold faster than the slowest phase in reduction at pH 8.5; thus, only the fast-reducing form (k_{red} = 7.0 s^{-1}) is participating significantly in turnover at this pH, though it is not the rate-determining step in catalysis. It is shown in Figure 9C that formation of oxidized flavin at pH 8.5 is a combination of reactions that correspond to the turnover number.

Oxidative Half-Reaction. The oxidative half-reaction of Ala45Gly-PHBH (k_5–k_{10} in Figure 1) was studied in detail. The anaerobic Ala45Gly enzyme reduced with dithionite and in complex with pOHB, at pH 6.5 and 4 °C, was mixed with buffer containing known concentrations of dissolved oxygen in a stopped-flow spectrophotometer. Absorbance changes were observed at wavelengths from 340 to 600 nm, and fluorescence changes were observed with excitation at both 390 and 450 nm with emission beyond 510 nm. The reaction was complex, but could be fitted with a consistent set of five rate constants over all wavelengths. The fluorescence traces with excitation at 390 nm (Figure 9A) clearly show the five phases. The first phase (see the increase in absorbance at 390 nm in the first 30 ms) was linearly dependent on oxygen concentration with a second-order rate constant of 1.2×10^5 M^{-1} s^{-1}. This phase (k_5 in Figure 1) is observed as a large increase in absorbance and a slight increase in fluorescence from that of the reduced enzyme at wavelengths from 340 to 420 nm, and is indicative of the formation of a flavin–C4a-hydroperoxide intermediate with a spectrum similar to that of the WT flavin–C4a-hydroperoxide. This hydroperoxide reacted in a first-order process with a rate constant of 1.3 ± 0.1 s^{-1}, illustrated by the large increase in fluorescence with excitation at 390 nm. This increase in fluorescence is accompanied by an increase in absorbance at 470 nm (between 0.3 and 5 s in Figure 9A) due to the simultaneous formation of a large proportion of oxidized enzyme. The increase in fluorescence is characteristic of formation of a flavin–C4a-hydroxide intermediate and indicates hydroxylation of pOHB (*13*). Thus, in this reaction, both C4a-hydroxyflavin and oxidized enzyme species are formed simultaneously from the C4a-hydroperoxyflavin intermediate. In identical half-reactions in which the reaction products were analyzed by HPLC, it was found that 57% of the reduced enzyme catalyzed hydroxylation to form 3,4DOHB. On the basis of these results, the rate constant for hydroxylation (k_6 in Figure 1) was calculated from the overall rate of breakdown of the flavin hydroperoxide to be 0.7 s^{-1} (60-fold slower than that of WT-PHBH under the same conditions) and the rate constant for breakdown of the C4a-hydroperoxyflavin to H_2O_2 and FAD (k_{10} in Figure 1) was calculated to be 0.6 s^{-1}.

The transient increase in the fluorescence signal observed with excitation at 390 nm (Figure 9A) that is due to the flavin hydroxide was concurrent with an increase in absorbance at 470 nm (Figure 9A), which indicates a simultaneous rapid formation of oxidized FAD following hydroxylation. The increase in fluorescence is the result of a small fraction of a highly fluorescent flavin–C4a-hydroxide formed in the hydroxylation reaction being trapped by pOHB after release of 3,4DOHB but before elimination of H_2O to re-form oxidized flavin. A similar trapping event has been shown to occur in the Pro293Ser mutant form of PHBH (*11*). This trapping of the 4a-hydroxyflavin occurs because the complex with pOHB loses water more slowly than the product complex. This conclusion is confirmed by the dependence of the rate of decrease of fluorescence (between 3 and 30 s in Figure 9A) being inversely proportional to the concentration of pOHB in the reaction mixture (e.g., 0.07 s^{-1} with 500 μM pOHB and 0.18 s^{-1} with 80 μM pOHB). The small changes seen with 390 nm fluorescence excitation at long times (a small increase and decrease with rates of 0.014 and

0.004 s^{-1}, respectively, in Figure 9A) correspond to a small amount of the observed absorbance change (5%) and are not dependent on pOHB or oxygen concentrations. These very slow phases are not involved in the measured turnover rate of the enzyme, which occurs at 0.06 s^{-1}.

The oxidative half-reaction was also studied at pH 8.5 and 4 °C (Figure 9B). At this higher pH, the rate constant for formation (1.4×10^5 M^{-1} s^{-1}) and the spectral properties of the flavin–C4a-hydroperoxide intermediate are similar to those observed at pH 6.5 and with the WT enzyme. However, decay of the hydroperoxide to the oxidized enzyme occurs in a biphasic reaction between 20 ms and 2 s (Figure 9B), unlike that observed at pH 6.5. Approximately 50% of the return to the oxidized enzyme (see A_{470}) occurs at a rate of 13 ± 2 s^{-1}, and can be attributed to enzyme that fails to hydroxylate substrate, since there is no corresponding fluorescence signal from excitation at 390 nm. A large increase in fluorescence with excitation at 390 nm between 30 and 200 ms occurs in a first-order process with a rate constant of 4 ± 0.5 s^{-1}. A spectrally silent step preceding this phase with a rate constant of ~15–20 s^{-1} is required (Figure 9C) to accurately simulate the fluorescence increases. There is no corresponding phase required in the absorbance traces, probably because the flavin–C4a-hydroxide and the flavin–C4a-hydroperoxide intermediates (Figure 1) have very similar absorbance spectra. The highly fluorescent flavin–C4a-hydroxide intermediate decays at a rate of 2.6 ± 0.2 s^{-1}, observed as a decrease in fluorescence between 200 ms and 2 s (Figure 9B), and this change corresponds to the second phase (~40% of the increase in absorbance) at 470 nm. This phase is attributed to the loss of water and product from the enzyme to re-form the oxidized enzyme, with simultaneous formation of the pOHB-trapped flavin–C4a-hydroxide intermediate. After most of the enzyme is oxidized, a final slow phase is observed as another small increase in absorbance at 470 nm between 2 and 20 s with an observed rate of 0.2 ± 0.02 s^{-1}; this accounts for ~10% of the total enzyme in the reaction. This final phase is slower than the measured turnover at pH 8.5 of 1.1 s^{-1}, and is most likely the fraction of the enzyme that is trapped as the flavin–C4a-hydroxide intermediate by the excess pOHB present, slowly releasing water to form the oxidized enzyme. A scheme summarizing this complex reaction is shown in Figure 9C. The amount of product formed at pH 8.5 in the oxidative half-reaction was measured by HPLC, and it was found that 0.55 mol of 3,4DOHB was formed for each mole of enzyme oxidized. Interestingly, in steady-state turnover at pH 8.5 and 4 °C, coupling of NADPH consumption (monitored spectrally at 340 nm) to production of 3,4DOHB (measured using HPLC) shows 90 ± 5% hydroxylation (Table 2). As has been demonstrated from comparison of turnover studies with studies of reduction of the enzyme by NADPH (above), only the fast-reducing form (~50% of the total) of the enzyme participates significantly in turnover, and this form is quite efficient in the hydroxylation reaction. The rate-limiting step in turnover at pH 8.5 for this mutant enzyme is the re-formation of oxidized enzyme after hydroxylation (see Figure 9C).

DISCUSSION

The dramatic and complex changes caused by the removal of a single methyl group demonstrate the highly interactive

structure of PHBH. These extensive changes from such a minimal substitution highlight the need for thorough study of variants in guiding the interpretation of mutagenesis experiments. We shall focus upon the relationship between the crystal structure and the properties of this remarkable mutant enzyme and what these observations can tell us about the function of PHBH.

Two Structures of Ala45Gly-PHBH. The results from the kinetics of reduction at pH 6.5 and 4 °C (Figure 7A) showed two distinct forms of Ala45Gly-PHBH, with the faster-reducing form constituting most of the enzyme. When the pH is increased to 8.5, reduction is much faster, with the fast and slow forms present in a ratio of 2.5:1, and a third phase was detected that was not dependent on NADPH concentration (Figure 8A). At pH 6.5, the fast-reducing form reduces 25-fold faster than the slow-reducing form, but this is nevertheless the slowest step in overall catalysis, and thus is the rate-limiting step in turnover (Table 2). The slower-reducing forms contribute very little to turnover at pH 6.5 or 8.5. Therefore, only the faster-reducing form of the Ala45Gly enzyme is a competent hydroxylase at pH 8.5. There is clear evidence from kinetics that two forms of the enzyme exist in solution and they interconvert slowly, as measured in pH-jump experiments (Figure 8B). Thus, it was gratifying to discover that the asymmetric unit of PHBH crystals that formed at pH 8.5 contained a dimer of the enzyme in which each monomer had a different conformation. The presence of an asymmetric dimer in the X-ray structure of Ala45Gly-PHBH hints that some form of half-sites catalysis occurs in the WT enzyme, similar to that shown in the case of thymidylate synthase (*29*). Thymidylate synthase is a homodimeric enzyme with confirmed half-sites reactivity, and under certain conditions, it forms crystals containing an asymmetric dimer that is important for enzyme function. However, there has been no kinetic evidence to suggest a half-sites model for any step in catalysis by WT-PHBH. The catalytically and structurally related enzyme, phenol hydroxylase, also crystallizes as an asymmetric homodimer structure (*30, 31*), with the FAD in one monomer *in* while the FAD in the other is *out*. However, there is no mechanistic evidence for half-sites reactivity for this enzyme. Another possible explanation for the crystallization of an asymmetric dimer that does not involve cooperativity between monomers is a selective crystallization of the predominant species out of solution. For instance, there could be a pool of dimers in solution where the monomer structures are in slow equilibrium between two forms, A or B, with each monomeric structure being independent of the structure of the other monomer on the dimer. Thus, when two different structural forms are equally likely to form, there will be a random collection of dimers with an A−A (25%), B−B (25%), or A−B (50%) structure. The A−B dimeric form would be the most likely to initiate nucleation of a crystal because of its higher concentration, similar to using crystallization as a purification technique, and also once the crystal form has been started with the dimers locked in the A−B form, the remaining homodimers in solution will equilibrate to form more A−B dimers that would again be preferentially added to the growing crystal over the two homodimeric forms, thus enriching the A−B form.

The faster-reducing form of Ala45Gly-PHBH at pH 8.5 is a competent hydroxylase, but the rate constant for

hydroxylation is 25-fold slower than that for WT. Hydroxylation by the Ala45Gly enzyme at pH 8.5 is ~7-fold faster than at pH 6.5. Thus, the faster form of the enzyme responds to the pK_a of the H-bond network in the WT-like structure. However, as described in the Results, the pK_a of the phenol of pOHB bound to the Ala45Gly enzyme (>9.0, Table 2) has shifted to a higher pH than with WT (pH 7.4). During hydroxylation, pOHB is deprotonated to the activated phenolate form in the transition state by the action of the H-bond network connected to His72 on the surface of the protein (*25*). With the Ala45Gly enzyme at pH 8.5, this activation is only partial because the pK_a values for pOHB bound to either form of the enzyme are >9.0 (Table 2). The high pK_a in the His72-flipped form of Ala45Gly-PHBH occurs because the H-bond network that facilitates deprotonation of pOHB is disrupted by removal of His72 from the proton transfer chain (Figure 4 B). The WT-like form of Ala45Gly-PHBH has a complete H-bond network, but the side chains of residues His72 and Gln213 have moved sufficiently close together (2.65 Å, not shown) for there to be a strong H-bond interaction between the two. Such a strong H-bond would affect the pK_a of His72, and as the terminal residue of the H-bond network, it would also affect both the pK_a of the H-bond network itself and the pK_a of the phenolic oxygen of bound pOHB.

Conformational States in Ala45Gly-PHBH. The *in* conformation of Ala45Gly-PHBH is more stable than the *out* or *open* conformation when compared to WT. When pOHB is bound to WT, it stabilizes PHBH in the *in* conformation at pH ≤7.0, with a characteristically low extinction coefficient and more resolved flavin spectrum (*17*). The Ala45Gly enzyme binds pOHB more tightly than does WT (Table 1) and exhibits a characteristic *in* flavin spectrum (Figure 6). Nevertheless, binding and release of pOHB probably require movement to the *open* conformation to allow diffusion of pOHB into or away from the active site (*3*). Binding of the product to Ala45Gly-PHBH, like pOHB binding, is significantly tighter than to WT (Table 2). Unlike WT (*32*), spectral perturbations upon binding of 3,4DOHB to Ala45Gly-PHBH are very similar to those shown for binding of pOHB (Figure 6). Thus, bound with either pOHB or product 3,4DOHB, the *in* conformation of Ala45Gly-PHBH is considerably more favorable than the other conformations. Because the *open* conformation is required for exchange of substrate and product, exchange is slow (L. J. Cole, unpublished results). By contrast, the *open* conformation in oxidized WT-PHBH is more easily attained, resulting in fast exchange of ligands (*33*).

The slow rate of reduction in catalysis by both forms of the Ala45Gly enzyme is also caused by the relative instability of the *out* conformation that is required for effective interaction with NADPH. The observation of a full deuterium kinetic isotope effect upon reduction of the competent form of the enzyme (Figure 7B) shows that the observed rate is indeed due to the chemical hydride transfer, rather than to a slow rate of conformational change from *in* to *out*. The explanation for the kinetic isotope effect is that the equilibrium strongly favors the *in* conformation so that at any given time only a small fraction of enzyme is in the *out* conformation where the isoalloxazine is reduced. As the pH is increased, the WT-like mutant enzyme responds to the H-bond network and the rate constant for reduction increases

100-fold between pH 6.5 and 8.5 (Figures 7A and 8A). Also consistent with this equilibrium argument is the fact that the Ala45Gly-PHBH binds 2,4DOHB less tightly than does the WT enzyme. When the WT enzyme binds 2,4DOHB, the isoalloxazine moves to the *out* conformation (*9, 17*). The weaker binding of 2,4DOHB to the variant is due to the *out* conformation being less favorable than in WT (Table 2).

The slower-reducing form of the Ala45Gly enzyme (that also fails to hydroxylate) shows only a small primary isotope effect (~2), indicating that this structural form may change between *in* and *out* conformations slowly, so that this process contributes to the very slow observed rate constant for reduction of this form and masks the kinetic isotope effect. This observation is consistent with the report of slow rates of change between the *in* and *out* conformations in forms of PHBH with a disrupted H-bond network (*25*). Thus, a combination of the stability of the *in* conformation and a disrupted H-bond network may explain the very slow reduction of the His72-flipped form of the enzyme.

Preferential stabilization of the *in* conformation with Ala45Gly-PHBH is consistent with the hypothesis put forward in the introductory section that the protein loop of PHBH on the *si* side of the flavin is vitally important for protein conformational change. Within the loop, Arg44 and Ala45 are probably the most important residues. With the structure of Ala45Gly-PHBH presented here and several other existing crystal structures of PHBH, a pattern of noncovalent interactions that affect conformational states of PHBH is emerging. An H-bond network among the carbonyl of Arg44, a crystal water, and the side chain of Arg220 found in the WT structure with pOHB bound [*in* conformation (*4*) (Figure 2)] is consistently disturbed when a mutation or substrate analogue favors another conformation. In the Arg220Gln form of PHBH, which stabilizes the *open* conformation (*3*), the backbone of Arg44 and Ala45 is rotated (Figure 2), to relieve an unfavorable backbone conformation of Arg44 (*16*). In the structure of the Arg220Gln enzyme with NADPH bound, the guanidinium group in the side chain of Arg44 charge-pairs to the 2′-phosphate of NADPH (*3*), showing that NADPH binding has a direct influence on this system. When pOHB is not bound to PHBH in the *open* structure, Arg214 is moved away from the active site (*3*) and no longer H-bonds to the carbonyl of Arg44 (Figure 2). This move results in less H-bonding to stabilize the strained Arg44 backbone. Thus, we propose that disruption of the Arg220 to Arg44 H-bond network favors rotation of the loop that contains Arg44 and Ala45 to relieve the unfavorable backbone conformation of Arg44, and this results in promotion of the *open* conformation. When pOHB binds to PHBH and Arg214 rotates in and binds the carboxylate of the substrate, Arg214 helps restrain the backbone carbonyl of Arg44, and the Arg44 and Ala45 backbone is held in the strained conformation. The more flexible double glycine structure consisting of Gly45 and Gly46 in Ala45Gly-PHBH has weakened the strains of the *in* conformation so that rotation of the *si* side loop to form the *open* conformation is less favored.

His72 in Ala45Gly-PHBH. The changes around His72 in the His72-flipped monomer occur approximately 14 Å from the position of the methyl group change in the structure (Figure 4) and demonstrate the highly interactive nature of the structure of PHBH. Because it is the residue at the solvent interface of the H-bond network that removes the phenolic proton of pOHB, His72 is vitally important to the function of PHBH (*6, 25, 27*). Structural changes similar to those near His72 in Ala45Gly-PHBH (that cause large effects upon catalysis as demonstrated in the results of this paper) might also occur in the WT enzyme during catalysis. For example, it has been observed in structures of the WT enzyme over a range of pH values, that His72 undergoes a rotation of its imidazole ring by 90° as the pH is shifted from 5.0 to 7.4 (*12*). Conformational changes to His72 might be important in disabling the H-bond network in the absence of pOHB, thus preventing flavin reduction when NADPH binds (as observed experimentally) by not favoring the *out* conformation. Protein rearrangements associated with the binding of pOHB would then re-establish the H-bond network, making flavin reduction possible.

Dimer Interface of Ala45Gly-PHBH. There is no evidence for any type of intermonomer cooperativity having a role in the function of PHBH in WT or mutant enzymes, though conversely very little has been done to study the function of homodimers in PHBH or other flavin monooxygenases. Ala45Gly-PHBH crystallizes as an asymmetric dimer. More importantly, the dimer shows asymmetry in the dimer interface itself, suggestive of a communication pathway between active sites. In the Ala45Gly-PHBH structure, Arg179 from the WT-like monomer is charge-paired to Asp357 from the His72-flipped monomer (Figure 5). However, like the WT-PHBH symmetrical structure, Arg179 from the His72-flipped monomer is not associated with Asp357 from the WT-like monomer. Arg179 is also a highly conserved residue (though Asp357 is not highly conserved) across PHBH sequences from many species, hinting at a more important role than simply a charged surface residue. Work to elucidate the role of the homodimer in the function of PHBH could be illuminating with respect to the function of this enzyme.

REFERENCES

1. Entsch, B., and van Berkel, W. J. (1995) Structure and mechanism of *para*-hydroxybenzoate hydroxylase, *FASEB J. 9*, 476−483.
2. Entsch, B., Cole, L. J., and Ballou, D. P. (2005) Protein dynamics and electrostatics in the function of *p*-hydroxybenzoate hydroxylase, *Arch. Biochem. Biophys. 433*, 297−311.
3. Wang, J., Ortiz-Maldonado, M., Entsch, B., Massey, V., Ballou, D., and Gatti, D. L. (2002) Protein and ligand dynamics in 4-hydroxybenzoate hydroxylase, *Proc. Natl. Acad. Sci. U.S.A. 99*, 608−613.
4. Schreuder, H. A., Prick, P. A. J., Wierenga, R. K., Vriend, G., Wilson, K. S., Hol, W. G. J., and Drenth, J. (1989) Crystal structure of *p*-hydroxybenzoate hydroxylase-substrate complex refined at 1.9 Å resolution, *J. Mol. Biol. 208*, 679−696.
5. Husain, M., and Massey, V. (1979) Kinetic studies on the reaction of *p*-hydroxybenzoate hydroxylase. Agreement of steady state and rapid reaction data, *J. Biol. Chem. 254*, 6657−6666.
6. Palfey, B. A., Moran, G. R., Entsch, B., Ballou, D. P., and Massey, V. (1999) Substrate recognition by "password" in *p*-hydroxybenzoate hydroxylase, *Biochemistry 38*, 1153−1158.
7. Palfey, B. A., Entsch, B., Ballou, D. P., and Massey, V. (1994) Changes in the catalytic properties of *p*-hydroxybenzoate hydroxylase caused by the mutation Asn300Asp, *Biochemistry 33*, 1545−1554.
8. Palfey, B. A., Ballou, D. P., and Massey, V. (1997) Flavin conformational changes in the catalytic cycle of *p*-hydroxybenzoate hydroxylase substituted with 6-azido- and 6-aminoflavin adenine dinucleotide, *Biochemistry 36*, 15713−15723.
9. Schreuder, H. A., Mattevi, A., Obmolova, G., Kalk, K. H., Hol, W. G., van der Bolt, F. J., and van Berkel, W. J. (1994) Crystal structures of wild-type *p*-hydroxybenzoate hydroxylase complexed

with 4-aminobenzoate, 2,4-dihydroxybenzoate, and 2-hydroxy-4-aminobenzoate and of the Tyr222Ala mutant complexed with 2-hydroxy-4-aminobenzoate. Evidence for a proton channel and a new binding mode of the flavin ring, *Biochemistry 33*, 10161−10170.

10. Ortiz-Maldonado, M., Entsch, B., and Ballou, D. P. (2003) Conformational changes combined with charge-transfer interactions are essential for reduction in catalysis by *p*-hydroxybenzoate hydroxylase, *Biochemistry 42*, 11234−11242.

11. Palfey, B. A., Basu, R., Frederick, K. K., Entsch, B., and Ballou, D. P. (2002) Role of protein flexibility in the catalytic cycle of *p*-hydroxybenzoate hydroxylase elucidated by the Pro293Ser mutant, *Biochemistry 41*, 8438−8446.

12. Gatti, D. L., Entsch, B., Ballou, D. P., and Ludwig, M. L. (1996) pH-dependent structural changes in the active site of *p*-hydroxybenzoate hydroxylase point to the importance of proton and water movements during catalysis, *Biochemistry 35*, 567−578.

13. Moran, G. R., Entsch, B., Palfey, B. A., and Ballou, D. P. (1997) Electrostatic effects on substrate activation in *para*-hydroxybenzoate hydroxylase: Studies of the mutant lysine 297 methionine, *Biochemistry 36*, 7548−7556.

14. Ortiz-Maldonado, M., Cole, L. J., Dumas, S. M., Entsch, B., and Ballou, D. P. (2004) Increased positive electrostatic potential in *p*-hydroxybenzoate hydroxylase accelerates hydroxylation but slows turnover, *Biochemistry 43*, 1569−1579.

15. Bruice, T. C., Noar, J. B., Ball, S. S., and Venkataram, U. V. (1983) Monooxygen Donation Potential of 4a-Hydroperoxyflavins As Compared with Those of a Percarboxylic Acid and Other Hydroperoxides. Monooxygen Donation to Olefin, Tertiary Amine, Alkyl Sulfide, and Iodide Ion, *J. Am. Chem. Soc. 105*, 2452−2463.

16. Eppink, M. H., Schreuder, H. A., and van Berkel, W. J. (1995) Structure and function of mutant Arg44Lys of 4-hydroxybenzoate hydroxylase: Implications for NADPH binding, *Eur. J. Biochem. 231*, 157−165.

17. Gatti, D. L., Palfey, B. A., Lah, M. S., Entsch, B., Massey, V., Ballou, D. P., and Ludwig, M. L. (1994) The mobile flavin of 4-OH benzoate hydroxylase, *Science 266*, 110−114.

18. Entsch, B., Palfey, B. A., Ballou, D. P., and Massey, V. (1991) Catalytic function of tyrosine residues in *para*-hydroxybenzoate hydroxylase as determined by the study of site-directed mutants, *J. Biol. Chem. 266*, 17341−17349.

19. Moran, G. R., and Entsch, B. (1995) Plasmid mutagenesis by PCR for high-level expression of *para*-hydroxybenzoate hydroxylase, *Protein Expression Purif. 6*, 164−168.

20. Entsch, B. (1990) *para*-Hydroxybenzoate hydroxylase, *Methods Enzymol. 188*, 138−147.

21. Press, W. H., Teukolsky, S. A., Vetterling, W. T., and Flannery, B. P. (1992) *Numerical Recipes in C. The Art of Scientific Computing*, 2nd ed., Cambridge University Press, Cambridge, U.K.

22. Brunger, A. T., Adams, P. D., Clore, G. M., DeLano, W. L., Gros, P., Grosse-Kunstleve, R. W., Jiang, J. S., Kuszewski, J., Nilges, M., Pannu, N. S., Read, R. J., Rice, L. M., Simonson, T., and Warren, G. L. (1998) Crystallography & NMR system: A new software suite for macromolecular structure determination, *Acta Crystallogr. D54*, 905−921.

23. Levitt, M., and Perutz, M. F. (1988) Aromatic rings act as hydrogen bond acceptors, *J. Mol. Biol. 201*, 751−754.

24. Steiner, T., Schreurs, A. M., Kanters, J. A., and Kroon, J. (1998) Water molecules hydrogen bonding to aromatic acceptors of amino acids: The structure of Tyr-Tyr-Phe dihydrate and a crystallographic database study on peptides, *Acta Crystallogr. D54*, 25−31.

25. Ortiz-Maldonado, M., Entsch, B., and Ballou, D. P. (2004) Oxygen reactions in *p*-hydroxybenzoate hydroxylase utilize the H-bond network during catalysis, *Biochemistry 43*, 15246−15257.

26. Eschrich, K., van der Bolt, F., de Kok, A., and van Berkel, W. J. H. (1993) Role of Tyr201 and Tyr385 in substrate activation by *p*-hydroxybenzoate hydroxylase from *Pseudomonas flourescens*, *Eur. J. Biochem. 216*, 137−146.

27. Frederick, K. K., Ballou, D. P., and Palfey, B. A. (2001) Protein dynamics and control in the reactions of *p*-hydroxybenzoate hydroxylase, *Biochemistry 40*, 3891−3899.

28. Gibson, Q. H., Swoboda, B. E. P., and Massey, V. (1964) Kinetics and mechanism of action of glucose oxidase, *J. Biol. Chem. 239*, 3927−3934.

29. Anderson, A. C., O'Neil, R. H., DeLano, W. L., and Stroud, R. M. (1999) The structural mechanism for half-the-sites reactivity in an enzyme, thymidylate synthase, involves a relay of changes between subunits, *Biochemistry 38*, 13829−13836.

30. Enroth, C. (2003) High-resolution structure of phenol hydroxylase and correction of sequence errors, *Acta Crystallogr. D59*, 1597−1602.

31. Enroth, C., Neujahr, H., Schneider, G., and Lindqvist, Y. (1998) The crystal structure of phenol hydroxylase in complex with FAD and phenol provides evidence for a concerted conformational change in the enzyme and its cofactor during catalysis, *Structure 6*, 605−617.

32. Spector, T., and Massey, V. (1972) Studies on the effector specificity of *p*-hydroxybenzoate hydroxylase from *Pseudomonas fluorescens*, *J. Biol. Chem. 247*, 4679−4687.

33. Entsch, B., Ballou, D. P., and Massey, V. (1976) Flavin-oxygen derivatives involved in hydroxylation by p-hydroxybenzoate hydroxylase, *J. Biol. Chem. 251*, 2550−2563.